Proceedings of the Second International Conference on Press-in Engineering 2021, Kochi, Japan – Matsumoto et al (eds)

Performance of pressed-in piles in saturated clayey ground: Experimental and numerical investigations

L.T. Hoang
Thuyloi University, Hanoi, Vietnam

X. Xiong & T. Matsumoto
Kanazawa University, Ishikawa, Japan

ABSTRACT: This paper investigates performance of pressed-in piles in saturated clay ground under isolated (SP) condition and pile group (PG) condition via both experimental and numerical methods. In the experiments, static load test (SLT) was conducted on one SP immediately and on another SP and PGs 24 hrs after the installation to investigate the consolidation effect on the pile capacity. The numerical analyses were conducted following the procedure of the model tests using PLAXIS 3D. The constitutive soil model called "soft soil creep model" was employed to describe the soil behaviors with parameters mainly obtained from laboratory element tests. The effect of the pile installation process on the ground stresses is simulated by cylindrical expansion. Both the measured and calculated results indicate that the ground consolidation significantly increases pile capacity, and the simulations results show a good agreement with the experimental results in terms of initial stiffness and pile shaft resistance.

1 INTRODUCTION

In foundation engineering, piles are well utilized as a foundation solution to support heavy structures or structures located on soft grounds, of which the settlements of shallow foundations are excessive for the allowable values or the bearing capacities of shallow foundations do not meet the design load. According to the construction method, piles are classified into two types: non-displacement piles, such as bored piles and pre-augered piles, and displacement piles, such as jacked-in piles and driven piles. It is widely accepted that the installation process makes a great difference in bearing capacity between two pile types (Deeks et al., 2005; Dijkstra, 2009).

The effects of the installation process on pile behavior were observed in many previous studies. When a pile is jacked into the ground, the soil will be displaced outwards from the pile with a volume equal to the pile volume, and the soil near the pile shaft is completely remodeled. The behavior of soil surrounding the pile depends on many factors such as the initial density, degree of saturation of the soil, or grain sizes. If the soil is a saturated cohesive soil with low permeability, the total stresses generated by the installation process in the soil surrounding the pile basically transfer to the pore water pressure (PWP) first. PWP generated during the installation period may equal or exceed the total overburden pressure and requires a duration after the installation process to dissipate and transfer into effective stress (Flaate, 1971; Bozozuk et al., 1978). A plastic zone is developed around the pile where the mobilized shear stress exceeds the original undrained shear strength of the soil. At the zone near the pile shaft, as the PWP dissipates with time during and after the installation process, the soil strength and stiffness increase, and the shear strength of the soil recover to an even higher value in magnitude than the initial value before piling (referred to as "side shear set-up" and "set-up effect"), which results in the change of pile performance with time (Cooke et al., 1979; Konrad and Roy, 1987; Whittle and Sutabutr, 1999; Svinkin and Skov, 2000; Bullock et al., 2005; Yan and Yuen, 2010; Basu et al., 2014). When such behavior of displacement piles is predicted more accurately, the design and construction of these piles will be more economically effective and safe.

The installation effect on the capacity of a pile in clay ground is currently analyzed by several methods. The total stress approach and the effective stress approach are the simplest methods, and they are commonly used in the current design. For these methods, pile resistance is calculated by an equation related to initial undrained shear strength s_u (Tomlinson, 1957), radial effective stress (Chow, 1997) or initial in-situ vertical effective stress σ'_{vo} (API-RP2A 1969) or a combination of both s_u and σ'_{vo}

DOI: 10.1201/9781003215226-10

(Ladd et al., 1977; Karlsrud et al., 2005). Since the fact that soil stiffness and soil strength change with time during and after the installation process, these calculated methods cannot take into account these changes. Another method for pile capacity prediction is based on cone penetration test (CPT)/piezocone penetration tests (CPTu). By this method, the pile shaft resistance is calculated by semi-empirical equations linked to the measurement results of cone tip resistance, PWP, and sleeve friction through a reduction factor (Nottingham, 1975; Almeida et al., 1996; Li et al., 2020). The reduction factor depends on pile shape, pile material, cone type, embedment ratio (Nottingham, 1975; Bustamante and Giaeselli, 1982), or measured cone shaft resistance (Clarke et al., 1993), or cone tip resistance and initial effective overburden stress (Almeida et al., 1996), or using an empirical value based on data from case histories (Eslami and Fellenius, 1997). Li et al. (2020) indicated that CPTu measurements could be a feasible approach to the estimation of the time-dependent bearing performance of jacked piles. In general, CPT/CPTu method has indicated as a reasonable approach to predict the bearing capacity of displacement piles. However, it should be noted that the empirical factors have been usually derived for particular regions (particular soil).

In recent times, a finite element analysis (FEA) is seen as an advanced and promising approach to model the pile installation effects. Some special code programs, such as Solid Nonlinear Analysis Code (SNAC) and Material Point Method (MPM), are developed to simulate the jacking and loading behavior of a pile; and the results showed reasonable agreements with measured results if appropriate soil parameters and constitutive model were selected (Basu et al., 2014; Lorenzo et al., 2018; Phuong, 2019). One disadvantage of these methods is that such programs are relatively complicated and uncommon. Therefore it is still difficult for designers to use these programs practically and straightforwardly. Some commercially available programs, such as PLAXIS and ABAQUS, are employed in several studies to model the behavior of jacked-in piles in clay ground in recent years (Engin, 2013; Engin et al., 2015; Lim et al., 2018; Khanmohammadi and Fakharian, 2019). In these studies, the pile installation process in clay ground was simulated under fully undrained conditions with a hypoplastic soil model (Engin, 2013; Engin et al., 2015) or Modified Cam-Clay model (Lim et al., 2018; Khanmohammadi and Fakharian, 2019). The above-mentioned studies paid attention to simulation techniques, parametric studies, or comparison with other calculation methods, however, a very limited number of studies utilized experimental results or field measurement data to validate the modeling.

In this study, the behaviors of jacked-in piles in saturated clay ground were investigated through both physical modeling and numerical modeling. For the numerical modeling, a standard available commercial package PLAXIS 3D was employed. The main aim of this study is to simulate the behavior of jacked-in piles using available software with simple techniques, to achieve practical and simple designs. The piles were investigated not only in isolated conditions but also in group conditions, and the results were compared with the corresponding experimental results. The focuses are on: i) load-settlement behavior of a single pile with and without considering the ground consolidation caused by the installation process; ii) load-settlement behavior of jacked piles in group conditions; iii) axial forces distributing along the pile. Furthermore, one more attempt for the modeling approach in this study is that almost the input soil parameters for the soil constitutive model were obtained directly from laboratory soil tests.

2 EXPERIMENTAL DESCRIPTION

2.1 *Model grounds*

Clay ground was prepared in a cylindrical chamber with a height of 420 mm and a diameter of 420 mm. The soil used for the model ground was a mixture of Kasaoka clay and Silica sand #6.

The model ground was prepared as follows: Firstly, Silica sand #3 was saturated and compacted in the chamber for a bottom drainage layer with a height of 50 mm, this drainage layer could be regarded as a rigid layer. Secondly, dry Kasaoka clay powder and Silica sand #6 were mixed at a mass ratio of 1:1 (K50S50) in a rectangular basin. Water was then added to the mixed soil to obtain a soil slurry with a water content of 1.3 *LL* (*LL*: liquid limit). This soil slurry was poured into the soil chamber to an initial thickness of 370 mm. The soil was left to consolidate under its self-weight for two days. After that, another Silica sand layer was placed on the clay to provide the top drainage layer, as shown in Figure 1. Next, a rigid circular loading plate was placed on the top drainage layer, and the vertical load on the loading plate was increased to consolidate the soil one-dimensionally in several steps up to vertical stress of 100 kPa. Each load step was maintained until the degree of consolidation reached 90% following Terzaghi's one-dimensional consolidation theory. The final load step was kept for one more week to reach a higher degree of consolidation. Finally, the consolidation pressure was removed and the ground was allowed for the swelling process in 10 days. After the swelling process, the thickness of the clay layer was 297 mm.

T-bar tests, cone penetration tests (CPTs), and unconfined compression tests (UCTs) were carried out immediately after completion of the load test on the piles to obtain properties of the model ground and to confirm the consistency between model grounds. The more details of the ground preparation, T-bar tests, CPTs, and UCTs were described in Hoang and

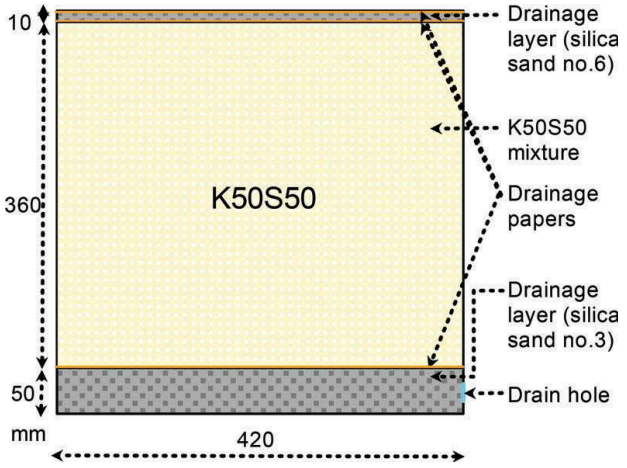

Figure 1. Preparation of model ground: longitudinal cross-sectional view before applying consolidation pressure.

Matsumoto (2020). A series of laboratory soil tests such as oedometer test, consolidated undrained (CU) triaxial compression test, Atterberg limits, density of soil particles were also carried out to obtain ground properties. Table 1 shows the properties of the model grounds. It is noted that effective cohesion c', tensile strength $\sigma_{t,}$ and Poisson's ratio for unloading/reloading ν_{ur} are not obtained from the above-mentioned soil tests (they are estimated/assumed values). However, they are also shown in the table because they are later used for the numerical analyses, together with the parameters obtained from the laboratory soil tests.

Table 1. Properties of model ground.

Soil parameter	Value
Density of soil particle ρ_s	2.653 Mg/m^3/g/cm^3
Plastic limit *PL*	13.6 %
Liquid limit *LL*	33.9 %
Plastic index *PI*	20.3 %
Compression index C_c	0.291
Swelling index C_s	0.055
Secondary compression index (creep index)C_α	0.00125
Effective cohesion *c'*	0.005 N/mm^2/5 kPa (estimated from simulations of CU test)
Friction angleϕ'	34.8 degrees
Tensile strength σ_t	0 (defaut)
Poisson's ratio for unloading/reloading ν_{ur}	0.17 (assumed)
Pre Overburden pressure *POP*	0.1 N/mm^2/100 kPa
Initial void ratio e_0	0.703
Permeability *k*	0.00038 mm/min
Change of permeability c_k	0.425
Unsaturated unit weight γ_{unsat}	0. 000019 N/mm^3
Saturated unit weight γ_{sat}	0. 000019 7 N/mm^3
Unit weight of water γ_{water}	0.00001 N/mm^3

* After completion of ground preparation.

2.2 *Model foundations*

Model piles used in the experiments were ABS (Acrylonitrile Butadiene Styrene) solid bars with a diameter *D* of 10 mm and a length *L* of 150 mm, as shown in Figure 2(a). Young's modulus E_p and Poisson's ratio ν of the model piles are 2920 N/mm^2 and 0.406, respectively. To measure axial forces along each pile, strain gages were attached on the pile shaft at different levels as shown in Figure 2(b). Model raft was a square aluminum plate with a thickness of 12 mm and a width *B* of 125 mm. The raft was regarded as a rigid raft.

In the experiments of single piles (SPs), the piles with 4 levels of strain gages were used. In the experiments of three group piles (PGs) with 4, 9, or 16 piles, the piles were arranged as shown in Figure 2 (c)-(e).

2.3 *Test procedure*

For the load test of SPs: Two SPs were jacked into the ground one by one with a center-to-center pile spacing of 20*D* (*D*: pile diameter) until the pile tip reached 140 mm below the ground surface. Static load test (SLT) was then conducted on one SP immediately and on another SP 24 hrs after the installation process to investigate the consolidation effect on the pile capacity. The rest period of 24 hrs is the necessary duration for the PWP generated during the installation process to dissipate (according to Hoang and Matsumoto, 2020).

For the load test of PGs: The load tests on three PGs with 4, 9, and 16 piles respectively and the same center-to-center pile spacing of 3*D* were carried out. In each PG, the piles were jacked into the ground one by one, after the pile installations, the raft was placed on the pile heads with a gap between the raft base and the ground surface of around 5 mm. The SLTs of PGs were then conducted 24 hrs after the completion of the pile installation.

Figure 3 shows the set-up of an experiment during the pile installation process and the SLT of a PG.

3 NUMERICAL SIMULATION

3.1 *Soil constitutive model*

Among available soil models in PLAXIS 3D (V20-CONNECTION), the Soft Soil Creep (SSC) model is the suitable model to describe the behavior of overconsolidated clayey soil considering the time effect. The detail of the SSC model is described in the material models manual of PLAXIS (PLAXIS 3D, 2018). To validate the soil model as well as to determine appropriate input soil parameters, simulation of CU triaxial test was conducted first. Almost

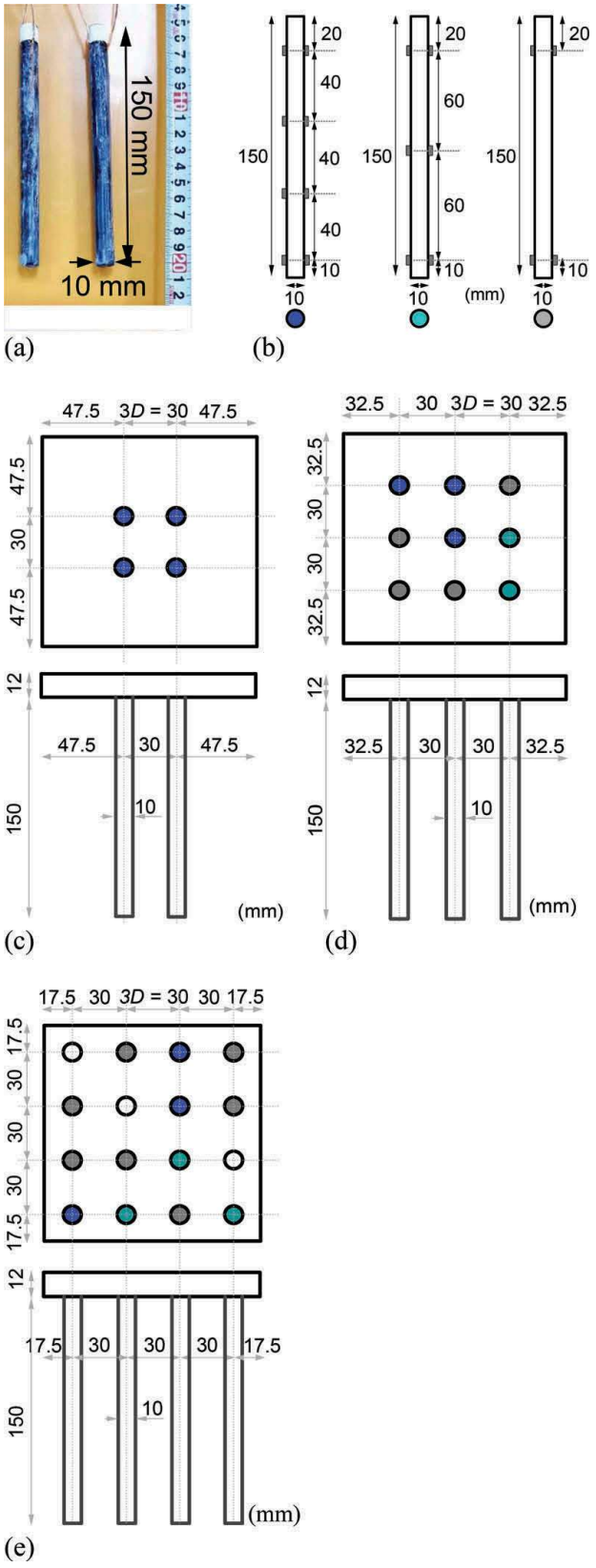

Figure 2. Model piles, raft, and pile foundation: (a) model piles; (b) locations of strain gages; (c) dimensions and arrangement of 4-pile pile group 4P-PG; (d) dimensions and arrangement of 9-pile pile group 9P-PG; (c) dimensions and arrangement o16-pile pile group 16P-PG.

all the input soil parameters were obtained from laboratory element tests, except for c', σ_t, and ν_{ur}

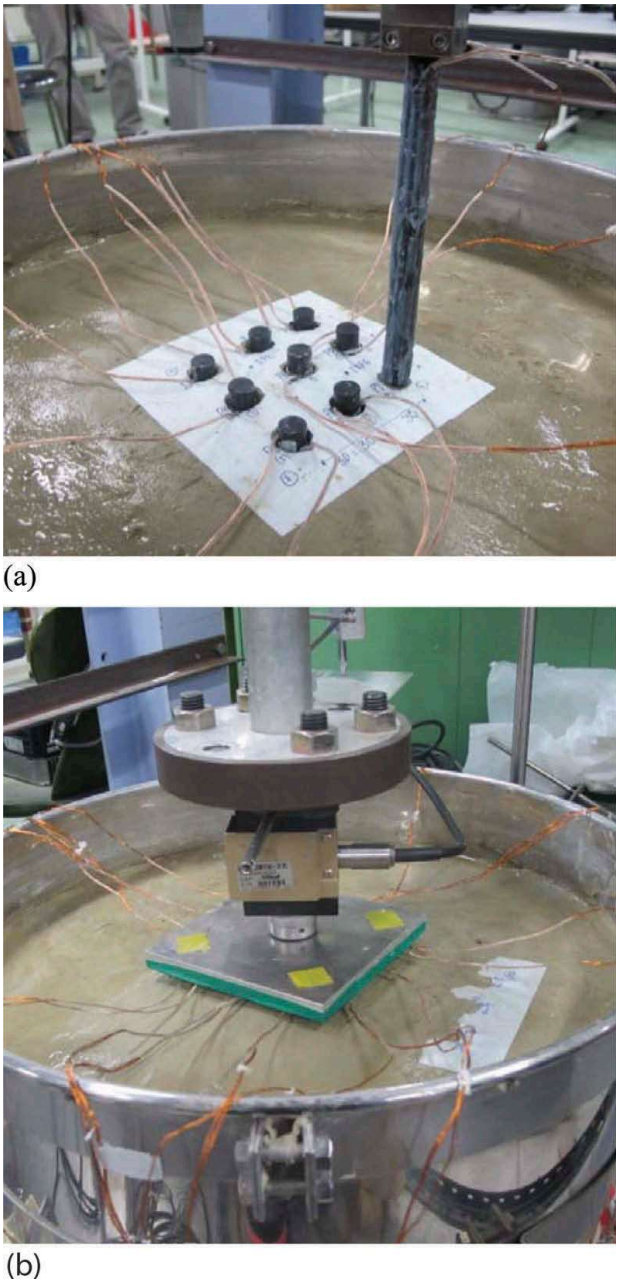

Figure 3. Set-up of an experiment during: (a) pile installation process; (b) SLT of a PG.

which were assumed/estimated values or set as default values. Table 1 shows the input soil parameters of the SSC model for the simulation of CU triaxial test $(C_c; C_s; C_\alpha; c'; \phi'; \sigma_t; \nu_{ur}; POP; e_0; k; c_k; \gamma_{unsat}; \gamma_{sat}; \gamma_{water})$. All geometry dimensions, drainage condition, consolidation time, shearing rate for the simulation followed the CU test in the laboratory. The analysis results of the CU triaxial test are shown and compared with measured results in Figures 4 and 5.

It is seen from Figure 4 that, in the consolidation stage, the trend of changes in volume strain was simulated quite well. Compared to the measured result, the changes in volume strain were a little higher at the initial consolidation process of each step. At the end of the consolidation stage, the

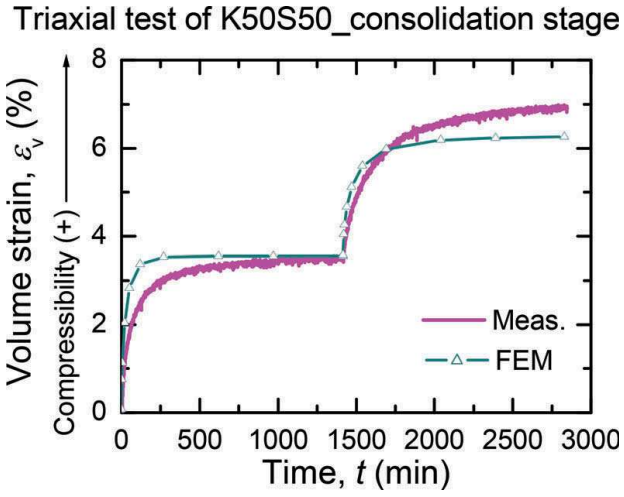

Figure 4. Change of volume strain during consolidation stage of CU triaxial test.

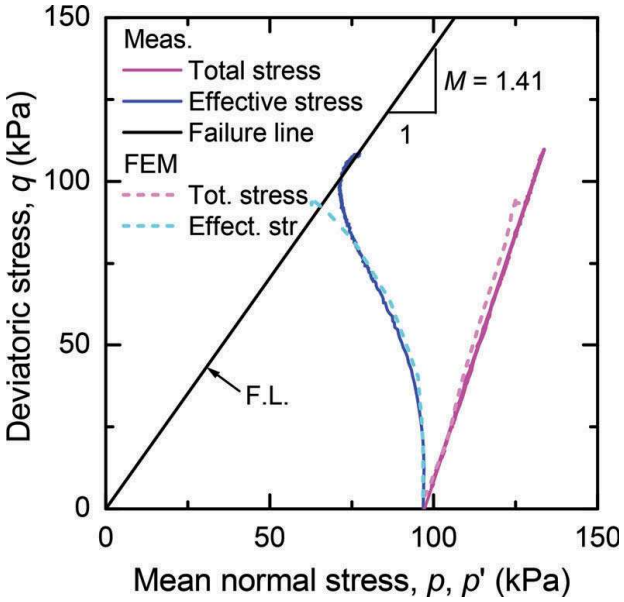

Figure 5. Normal stress versus deviatoric stress during axial compression stage of CU test.

calculated volume strain reached about 90% of the measured result.

Figure 5 shows the comparisons of total stress paths and effective stress paths between simulated and measured results in the undrained shearing stage. The relationship between effective mean normal stress p' and deviatoric stress q was simulated well from the start of the shearing stage until the failure state was nearly reached.

In general, the SSC model with the input parameters basically obtained from laboratory element tests can reasonably simulate the CU triaxial test. Therefore, in the next step, the SSC model and the same soil parameters are employed to simulate pile load tests.

3.2 *Numerical setup*

The FEM program PLAXIS 3D V20 CONNECTION implements a fully automatic generation of finite element meshes. The basic soil elements are the 10-node tetrahedral elements. For beam elements, 3-node line elements are used. Figure 6 shows the mesh for the calculations.

For the piles, the pile body is considered as linear elastic non-porous material (L.E.). A hybrid model of which beam elements surrounded by solid volume elements was employed to model the piles, according to Kimura and Zhang (2000). The main advantage of the hybrid pile modeling is that it is easier to obtain axial forces and bending moments along piles. In this research, the beam element of the hybrid pile model carried 90% of the bending stiffness EI and axial stiffness EA of the pile. The stiffness of the surrounding solid volume elements of the hybrid pile was reduced to 10% of the actual value, however, it was still much higher than the stiffness of the soil surrounding the pile. Table 2 shows the hybrid-pile model parameters.

Interface elements were set between the pile and the surrounding soil to model the pile-soil interaction. The properties of the interface elements are described by the strength properties of the surrounding soil with the application of an interface reduction factor R_{inter}. To determine an appropriate magnitude of R_{inter}, a series of simple experiments on piles slipping on the air-dry K50S50 ground was conducted; and the results show that the piles started to slip on the ground at an average incline angle of 31.2°(= 0.9 times of 34.8° of internal effective friction angle of K50S50 ground). The value R_{inter} = 0.9, therefore, was used for the analyses. It is noted that in the model test, the ground soil is saturated. However, R_{inter} was determined from the tests on dry ground because R_{inter} is defined in terms of effective stress in PLAXIS. Hence, the slip test on the dry ground is reasonable.

The geometry followed experiments, however, in numerical modeling, only 1/4 of the physical modeling was simulated owing to symmetric conditions. A groundwater table was set on the ground surface which is the same as the experiments. Figure 6 shows the geometry of the analyses.

In this paper, the pile installation effect was modeled by the cavity expansion method. This

Table 2. Parameters of the elastic elements.

Description	Beam	Solid pile	Raft
Material model		L.E.	L.E.
Unit weight γ (N/mm^3)	10.52×10^{-6}	1.169×10^{-6}	78.8×10^{-6}
Young's modulus, E (N/mm^2)	2628	292	200×10^3
Poisson's ratio ν	-	0.406	0.3

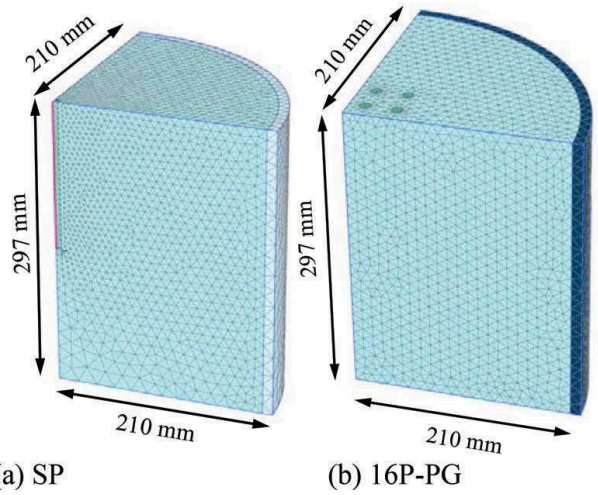

Figure 6. Mesh and geometry: (a) modeling of a single pile; (b) modeling of a pile group 16P-PG.

method has been previously used with PLAXIS by Broere and van Tol (2006) to model the bearing capacity of displacement piles in sand. The effect of the pile installation process on the ground stresses was simulated simply by prescribing volumetric strains on volume elements in the area representing the pile (see Broere and van Tol (2006) for more details of the simulation method). Several simulations with different values of volume strains were conducted first on SPs to select an appropriate strain value. This value is then used to simulate PGs. One another simulation scheme in this study is combining cylindrical cavity expansion with an amount of vertical displacement of 0.1D at the same time. The aim of using vertical displacement is to increase pile tip resistance due to pre-vertical pressure.

The analyses of pile load tests include: (i) SLT of SP was conducted immediately after installation, using volume expansion alone; (ii) SLT of SP was conducted immediately after installation, using volume expansion combine with vertical displacement; (iii) SLT of SP was conducted 24 hrs after installation, using volume expansion alone; (iv) SLT of SP was conducted 24 hrs after installation, using the combination of volume expansion with vertical displacement; (v) SLT of PGs was conducted 24 hrs after installation, using both volume expansion alone and combination of volume expansion with vertical displacement.

4 RESULTS AND DISCUSSIONS

4.1 *Load-settlement behavior of single piles in SLT conducted immediately after installation*

Figure 7 shows the load-settlement behavior during SLT of SP, of which SLT was conducted immediately after pile installation. Both measured and calculated results are shown in the figure.

Looking at Figure 7(a) first, the pile installation effect is simulated by the volume expansion scheme. The measured result shows that the pile head load reached a peak of about 125 N at a settlement of 0.75 mm. After that pile load reduced slightly and reached a residual capacity of around 121 N. The simulation result shows that when no expansion is applied ($\varepsilon_{xx} = \varepsilon_{yy} = 0\%$), the calculated pile bearing capacity is far below the measured result (about 70 N). However, when a small value of volume strain $\varepsilon_{xx} = \varepsilon_{yy} = 2.5$ % was applied, the calculated pile capacity increases effectively to about 97 N, and the pile capacity increases to 104 N when applying $\varepsilon_{xx} = \varepsilon_{yy} = 5.0$ %. Interestingly, when strains (ε_{xx}, ε_{yy}) are larger than 5.0%, the calculated pile bearing capacity was almost unchanged. It is thought that at the initial state just after volume expansion (the consolidation has not taken place), a small amount of lateral strain (ε_{xx}, $\varepsilon_{yy} > 5.0$ %) is enough to fully mobilize the shear strength of soil at the zone surrounding the pile shaft. Therefore, the calculated pile bearing capacity (of which SLT is carried out immediately after expansion) does not increase when applying larger lateral strain.

Figure 7(b) shows the results for the case of which the combination between volume expansion and vertical displacement of 0.1D was used for simulating the pile installation effect. Compared to Figure 7(a), at the same lateral strain, the pile capacity was almost unchanged when the vertical displacement is added, however, the initial stiffness of the load-settlement curve increased slightly. In both schemes shown in Figure 7, the calculated results were still smaller than the measured one.

In general, when simulating the installation effect of piles in saturated clay ground without consolidation after installation, a small amount of volume strain could increase pile resistance effectively and pile resistance becomes much closer to the measured result, in comparison with no expansion case.

4.2 *Load-settlement behavior of single piles in SLT conducted 24 hrs after installation*

Figure 8 shows the load-settlement behavior during SLT of SP, of which SLT was conducted 24 hrs after pile installation. The period of 24 hrs is necessary for the PWP generated during the installation process to completely dissipate (according to Hoang and Masumoto, 2020). Both measured and calculated results are shown in the figure for comparison.

The measured result in Figure 8 shows that the pile head load reached a peak of about 170 N at a settlement of 0.75 mm. After that pile load reduced slightly and reached a residual capacity of 150 N. Compared with the pile resistance at the time immediately after installation (Figure 7), the pile resistance after consolidation significantly increases by 25% (from 121 N to 150 N). The pile resistance increased because the PWP dissipated with time, the strength and stiffness of soil increased, and the shear

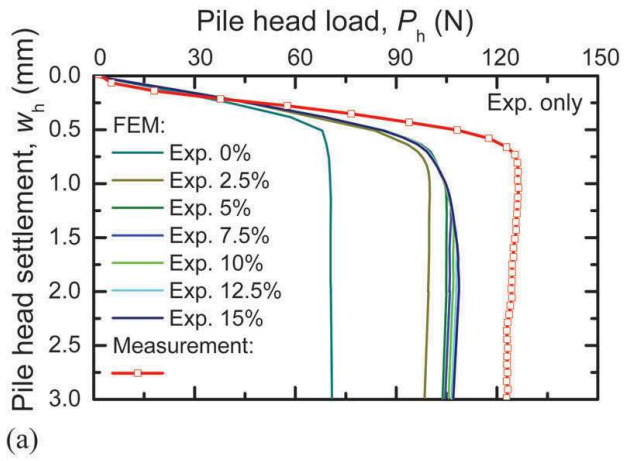

Figure 7. Load-settlement behavior of SP immediately after pile installation: (a) volume expansion alone; (b) combination of volume expansion with vertical displacement.

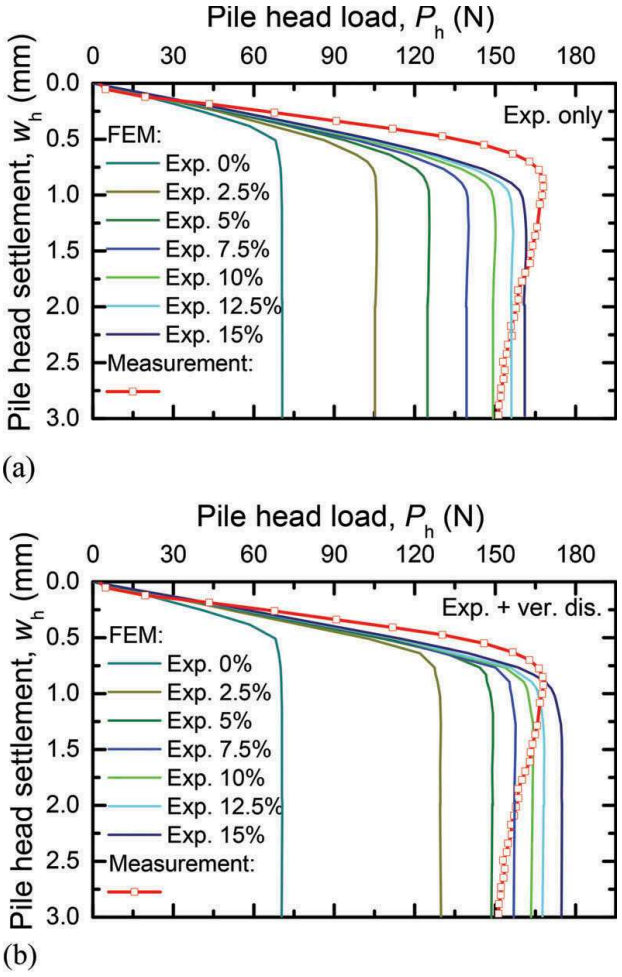

Figure 8. Load-settlement behavior of SP 24 hrs after pile installation: (a) volume expansion alone; (b) combination of volume expansion with vertical displacement.

strength of the soil recovered. This is commonly known as the set-up effect.

Figure 8(a) shows the results of SLTs of SP when the installation effect was simulated by volume expansion alone. Obviously, there is no change in pile resistance in case of no expansion. For the cases where the volume expansion was applied, the pile resistance increased significantly after the consolidation process (compared with Figure 7(a)), and the pile resistance increases as the magnitude of volume expansion increases. The value $\varepsilon_{xx} = \varepsilon_{yy} = 12.5$ % gives a good agreement between measured and calculated results at residual state.

Figure 8(b) shows the results of SLTs of SP when the installation effect is simulated by combining volume expansion (ε_{xx}, ε_{yy}) with vertical displacement (u_z). When vertical displacement was added, the pile resistance increased significantly. The combination of $\varepsilon_{xx} = \varepsilon_{yy} = 7.5$ % and $u_z = 0.1D$ gives a good agreement with measured result. The initial stiffness of load-settlement behavior also increases when u_z is added.

In general, both the experimental and numerical results indicated that the pile resistance increases significantly due to the soil consolidation caused by the pile installation. The addition of vertical displacement has a clear influence on the cases of simulation of SLTs after the consolidation, although it shows negligible influence on the cases of SLTs immediately after the pile installation.

4.3 *Load-settlement behavior of pile groups*

Figure 9 shows the load-settlement behavior during SLT of three PGs, of which SLTs were conducted 24 hrs after the completion of pile installation. In each figure, the measured result and the calculated results with both schemes are shown.

The results of all three PGs show that the initial stiffnesses are simulated quite well, both schemes give quite similar results. Regarding the magnitude of the group resistance, the resistance of 4P-PG is calculated reasonably. However, when the number of piles in the group increased, the calculated resistance was under the estimated one. This phenomenon may be explained by the differences in measured results and calculated results of load distributions between the pile tip and pile shaft. Further study is needed for this aspect. It is seen from Figure 9(a)-(c) that the differences between

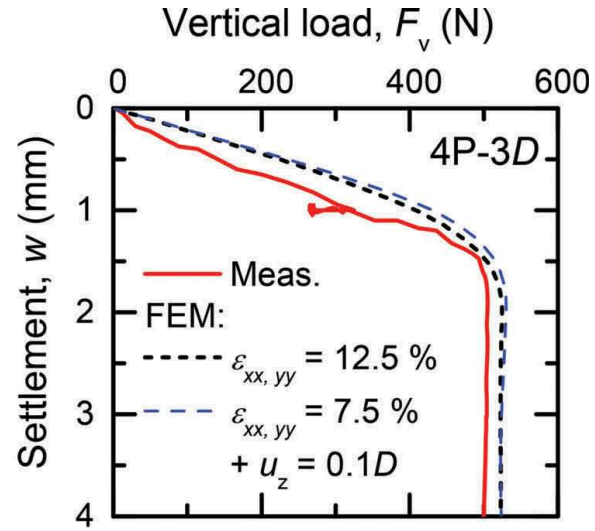

(a)

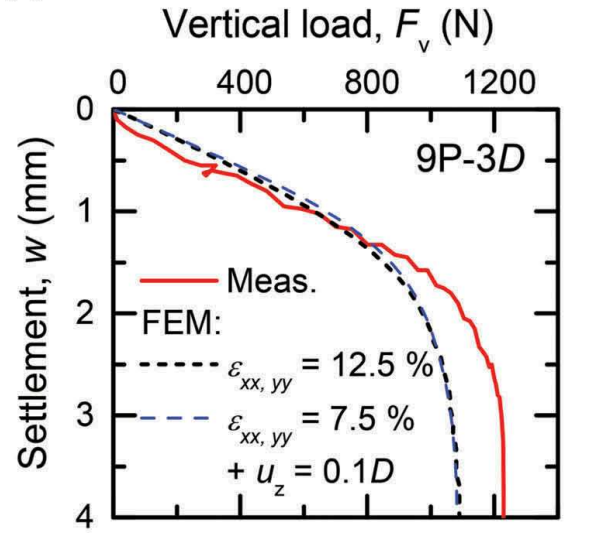

(b)

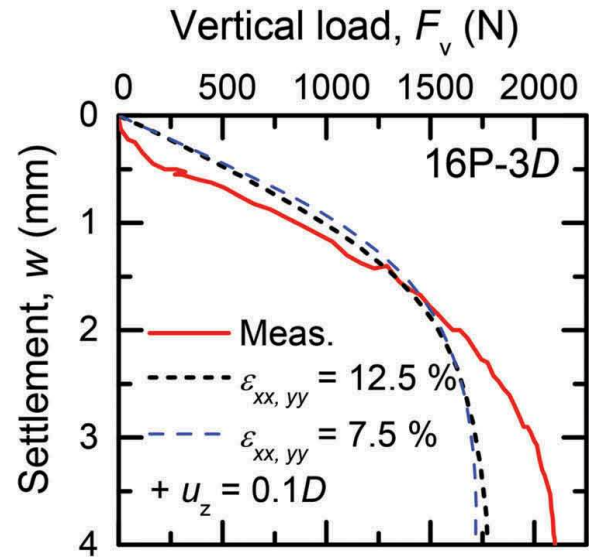

(c)

Figure 9. Load-settlement behavior of three PGs: (a) 4P-PG; (b) 9P-PG; (c) 16P-PG.

the calculated results of the two schemes are negligible.

4.4 *Distributions of axial force along piles*

The distributions of axial force along SPs are shown in Figure 10 for the case of the SLTs conducted immediately after the pile installation. The distributions of axial forces are presented at different settlements (in form of settlement normalized by pile diameter *w*/*D*).

Figure 10(a) compares the measured results with the calculated results in the case of simulating the pile installation effect by using only the volume expansion. It is seen from the figure that the shaft resistances of the SP are simulated well at depths deeper than 60 mm. At the depths between the pile head and 60 mm from the pile head, the calculated shaft resistance is larger than the measured one. The

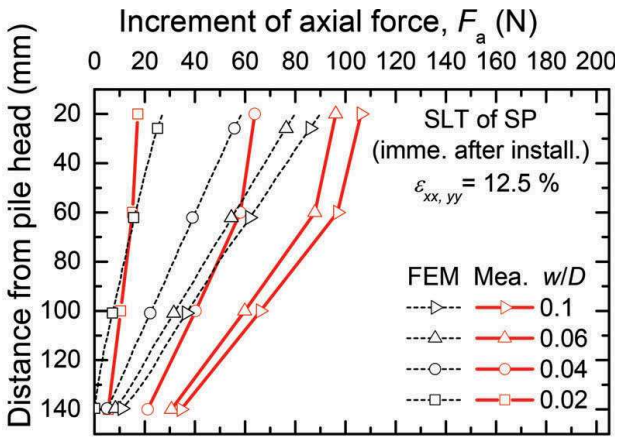

(a)

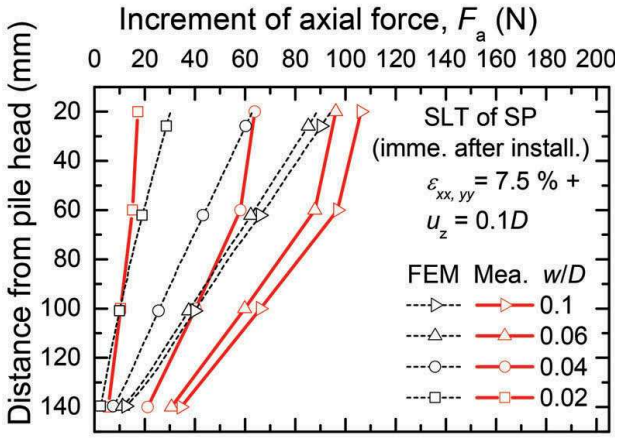

(b)

Figure 10. Distribution of axial force along piles when SLTs are conducted immediately after pile installation: (a) pile installation effect is simulated by volume expansion method; (b) pile installation effect is simulated by a combination of volume expansion method with vertical displacement.

calculated tip resistance is noticeably smaller than the measured values.

Figure 10(b) compares the measured results with the calculated results in the case of simulating the pile installation effect by using the combination of volume expansion with vertical displacement. It is found that the results in Figure 10(b) are very similar to the results in Figure 10(a). The addition of vertical displacement seems to have a slight effect on pile resistance as well as distributions of axial forces along the pile.

Figure 11 shows the distributions of axial force along SPs for the case of the SLTs conducted 24 hrs after pile installation in the cases: (a) pile installation effect is simulated by volume expansion method and (b) pile installation effect is simulated by a combination of volume expansion method with vertical displacement. It is found from the figure that at the small settlement (w/D = 0.02), the calculated axial force is larger than the measured one.

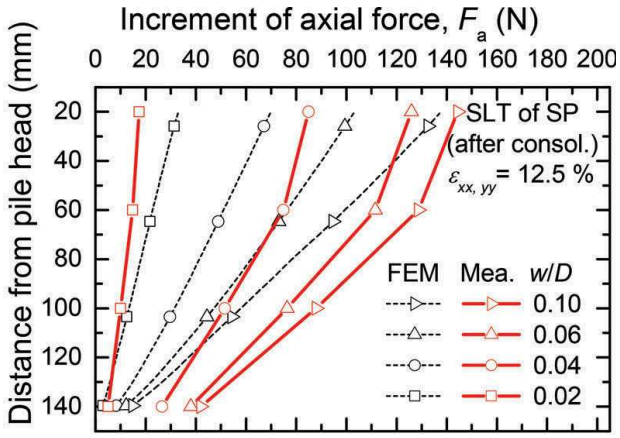

(a)

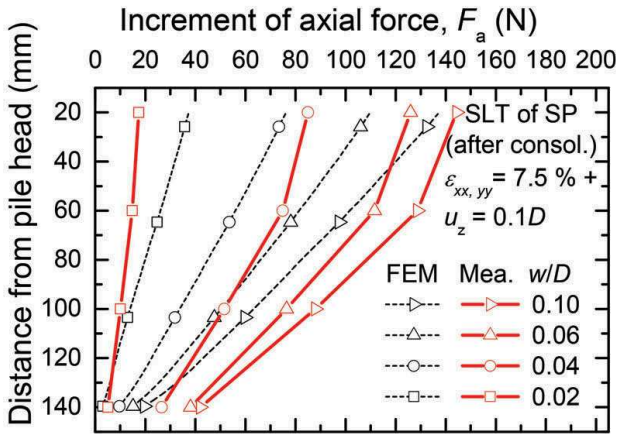

(b)

Figure 11. Distribution of axial force along piles when SLTs were conducted 24 hrs after pile installation: (a) pile installation effect is simulated by volume expansion method; (b) pile installation effect is simulated by a combination of volume expansion method with vertical displacement.

The results also show that shaft resistances are simulated well at depths deeper than 60 mm meanwhile the pile shaft resistances were overestimated at the top sections. The calculated tip resistance is noticeably smaller than the measured one. The tip resistance in the case of addition of vertical displacement (Figure 11(b)) is slightly higher, compared to the case of cylindrical cavity expansion alone (Figure 11(a)).

Comparing the measured axial forces along piles obtained from SLTs conducted before (Figure 10) and after (Figure 11) consolidation, the increment of pile resistance is mainly due to the increment of pile shaft resistance. The increment of tip resistance is minor.

The calculated results of two schemes show that the addition of vertical displacement has influences on pile shaft resistance rather than on pile tip resistance (as the amount of lateral strain reduces from 12.5 % to 7.5 %, however, the tip resistance does not increase much). Based on the measured results, several previous studies also pointed out that the installation process of a pile in saturated clay ground affects pile shaft resistance rather than pile tip resistance (Attwooll et al., 1999; Bullock et al., 2005). Therefore the reason for the underestimation of tip resistance and overestimation of shaft resistance near the pile top might be the use of a constant effective cohesion c' in analyses. If c' increases with depth, the more reasonable analysis results may be obtained.

5 CONCLUSION

This paper investigates behaviors of pressed-in piles in saturated clay ground under isolated and group conditions via both experimental and numerical methods. The following remarks are derived from the study:

The pile shaft resistance increased significantly after the soil consolidation, in comparison with the pile shaft resistance obtained from SLT conducted immediately after pile installation without consolidation.

Simulating the pile installation effect by the volume expansion method: When conducting SLT immediately after pile installation, a small value of lateral strain (reference value in this study: $\varepsilon_{xx} = \varepsilon_{yy} \geq 5.0$ %) is enough to fully mobilize the pile shaft resistance, and the pile resistance does not increase as the lateral strains increase. When conducting SLT after the consolidation process, the pile resistance increases as the lateral strains increase, and $\varepsilon_{xx} = \varepsilon_{yy} \approx 12.5$ % are appropriate strains for the case in this study.

Simulating pile installation effect by combination of volume expansion with vertical displacement: When conducting SLT immediately after pile installation, the addition of vertical displacement makes a slight increase in initial stiffness,

however, the residual resistance of pile is almost unchanged, compared with the case of applying volume expansion alone. When conducting SLT after the consolidation process, the pile resistance increases as the lateral strains increase and $\varepsilon_{xx} = \varepsilon_{yy} \approx 7.5$ % are appropriate strains for the case in this study. The addition of vertical displacement in the simulation of the pile installation effect increases pile resistance noticeably, in comparison with applying volume expansion purely. Interestingly, a large amount of the increment of pile resistance caused by the addition of vertical displacement is the increment of pile shaft resistance, not pile tip resistance. Other schemes should be done to increase the resistance of the pile tip.

In general, the installation effect could be simply simulated by applying volume strains before SLTs, although there are some differences between calculated and measured results. The pile set-up effects are also simulated reasonably by this method.

REFERENCES

Almeida, M.S.S., Danziger, F.A.B. & Lunne, T. 1996. Use of the piezocone test to predict the axial capacity of driven and jacked piles in clay. *Canadian Geotechnical Journal* 33(1),23–41. https://doi.org/10.1139/t96-022.

API (1969) Recommended practice for planning, designing, and constructing fixed offshore platforms, *API RP2A*, 1st edn. American Petroleum Institute, Washington

Attwooll, W.J., Holloway, D.M., Rollins, K.M., Esrig, M.I., Sakhai, S. & Hemenway, D. 1999. Measured pile setup during load testing and production piling: I-15 corridor reconstruction project in Salt lake city, Utah. Transportation research record, *Journal of the Transportation Research* 1663(1). https://doi.org/10.3141/1663-01

Basu, P., Prezzi, M., Salgado, R. & Chakraborty, T. 2014. Shaft resistance and setup factors for piles jacked in clay. *Journal of Geotechnical and Geoenvironmental Engineering* 140(3), 04013026. https://doi.org/10.1061/(ASCE)GT.1943-5606.0001018

Bozozuk, M., Fellenius, B.H. & Samson, L. 1978. Soil disturbance from pile driving in sensitive clay. *Canadian geotechnical journal* 15(3),346–361. https://doi.org/10.1139/t78-032

Broere, W. & van Tol, A. F. 2006. Modelling the bearing capacity of displacement piles in sand. *In Proc. of the Institution of Civil Engineers, Geotechnical Engineering* 159 (ICE, GE3), 1–13.

Bullock, P.J., Schmertmann, J.H., McVay, M.C. & Townsend, F.C. 2005. Side shear setup. I: Test piles driven in Florida. *Journal of Geotechnical and Geoenvironmental Engineering* 131(3),292–300. https://doi.org/10.1061/(ASCE)1090-0241(2005)131: 3

Bustamante, M. & Gianeselli, L. 1982. Pile bearing capacity prediction by means of static penetrometer CPT. *In Proc. of the 2nd European symposium on penetration testing*, Amsterdam, 493–500

Chow, F.C. 1997. Investigations into the behavior of displacement piles for offshore foundations. *PhD Thesis , Imperial College London, United Kingdom*.

Cooke, R.W., Price, G. & Tarr, K. 1979. Jacked piles in London Clay: a study of load transfer and settlement under working conditions. *Geotechnique* 29 (2), 113–147. https://doi.org/10.1680/geot.1979.29.2.113

Clarke, J., Long, M.M. & Hamilton, J. 1993. The axial tension test of an instrumented pile in overconsolidated clay at Tilbrook Grange. *In book: Large-scale pile tests in clay. Thomas Telford*, London, 362–380

Deeks, A., White, D. & Bolton, M. 2005. A comparison of jacked, driven and bored piles in sand. *In Proc. of the 16th International Conference on Soil Mechanics and Geotechnical Engineering* 4, pp. 2103–2106.

Dijkstra, J. 2009. On the modeling of pile installation. *Phd thesis of Technical University Delft,Netherlands*.

Eslami, A. & Fellenius, B.H. 1997. Pile capacity by direct CPT and CPTu methods applied to 102 case histories. *Can Geotech J* 34(6),886–904. https://doi.org/10.1139/t97-056

Engin, H.K. 2013. Modelling Pile Installation Effects – A Numerical Approach. *Ph. D. thesis, Geo-Engineering Section Delft University of Technology, The Netherlands*. DOI: 10.4233/uuid:3e8cc9e2-b70c-403a-b800-f68d65e6ea85

Engin, H.K., Brinkgreve, R.B.J. & van Tol, A.F. 2015. Simplified numerical modelling of pile penetration – the Press-Replace technique. *International Journal for Numerical and Analytical Methods in Geomechanics* 39 (15),1713–1734. https://doi.org/10.1002/nag.2376

Flaate, K. 1971. Effects of Pile Driving in Clays. *Canadian Geotechnical Journal* 9(1), pp. 81–88. https://doi.org/10.1139/t72-006

Hoang, L.T. & Matsumoto, T. 2020. Long-term behavior of piled raft foundation models supported by jacked-in piles on saturated clay. *Soils and Foundations* 60(1),198–217. https://doi.org/10.1016/j.sandf.2020.02.005

Karlsrud, K., Clausen, C.J.F. & Aas, P.M. 2005. Bearing capacity of driven piles in clay, the NGI approach. *In: Proc. of frontiers in offshore geotechnics: ISFOG, Perth*, pp 775–782. https://doi.org/10.1201/NOE0415390637.ch88

Khanmohammadi, M. & Fakharian, K. 2019. Numerical modelling of pile installation and set-up effects on pile shaft capacity. *International Journal of Geotechnical Engineering* 13(5),484–498. https://doi.org/10.1080/19386362.2017.1368185

Kimura, M. & Zhang, F. 2000. Seismic evaluations of pile foundations with three different methods based on three-dimensional elasto-plastic finite element analysis. *Soils and Foundations* 40(5),113–132.

Konrad, J. M. & Roy, M. 1987. Bearing capacity of friction piles in marine clay. *Geotechnique* 37(2),163–175. https://doi.org/10.1680/geot.1987.37.2.163

Ladd, C.C., Foott, R., Ishihara, K., Schlosser, F. & Poulos, H.G. 1977. Stress-deformation and strength characteristics, state-of the-art report. *In: Proc. of the International conference on soil mechanics and foundation engineering*, Tokyo, 421–494.

Li, L., Li, J., Sun, D. & Gong, W. 2020. A feasible approach to predicting time-dependent bearing performance of jacked piles from CPTu measurements. *Acta Geotechnica* 15, 1935–1952. https://doi.org/10.1007/s11440-019-00875-x

Lim, Y.X., Tan, S.A. & Phoon, K.K. 2018. Numerical study of pile setup for displacement piles in cohesive soils. *In: Cardoso et al. (Eds) Numerical Methods in Geotechnical Engineering IX*, Volume 1, 451–456, Taylor & Francis

Group, London. https://doi.org/10.1201/9780429446931 (ISBN 978-1-138-33198-3, viewing online on google book, no hard coppy or pdf version)

Lorenzo, R., Cunha, R.P., Cordao-Neto, M.P. & Naim, J.A. 2018. Numerical simulation of installation of jacked piles in sand using material point method. *Canadian Geotechnical Journal* 55(1),131–146. https://doi.org/10.1139/cgj-2016-0455

Nottingham, L.C. 1975. Use of quasi-static friction cone penetrometer data to estimate capacity of displacement piles. *PhD thesis of Department of Civil Engineering, University of Florida*, Gainesville, America.

Phuong, N.T.V. 2019. Numerical Modelling of Pile Installation Using Material Point Method. *PhD thesis*, *Delft University of Technology*, https://doi.org/10.4233/uuid:5580c747-d8a1-464c-8db8-e16eb2a499f7

PLAXIS 3D 2018 - Material Models Manual, PLAXIS, https://www.plaxis.com/support/manuals/plaxis-3d-manuals/

Svinkin, M. R. & Skov, R. 2000. Set-up effect of cohesive soils in pile capacity. *Proc., 6th Int. Conf. Application of Stress Wave Theory to Piles, S. Niyama and J. Beim, eds*., Balkema, Rotterdam, Netherlands, 107–111.

Tomlinson, M.J. 1957. The adhesion of piles driven in clay soils. *In: Proc. of the 4th international conference on soil mechanics and foundation engineering*, London.

Whittle, A.J. & Sutabutr, T. 1999. Prediction of pile setup in clay. *Journal of the Transportation Research Board* 1663(1),33–40. https://doi.org/10.3141/1663-05

Yan, W.M. & Yuen, K.V. 2010. Prediction of pile set-up in clays and sands. *IOP conf. series: Materials Science and Engineering* 10. https://doi.org/10.1088/1757-899X/10/1/012104